

# Periodic modulation effect and entanglement in hybrid optomechanical system containing a single quantum dot.

Vijay Bhatt<sup>1</sup>, Pradip K. Jha<sup>1</sup>, Aranya B. Bhattacharjee<sup>2</sup>, Souri Banerjee<sup>2</sup>

<sup>1</sup>*Department of Physics, DDU College,*

*University of Delhi, New Delhi 110078, India and*

<sup>2</sup>*Department of Physics, Birla Institute of Technology and Science,*

*Pilani, Hyderabad Campus, Hyderabad - 500078, India*

We theoretically study a parametrically modulated hybrid optomechanical system and propose a simple and efficient setting for the quantum control of the system dynamics. We explore this modulation regime by modulating two parameters simultaneously over time, the quantum dot (QD) frequency and the laser pump amplitude. We show that the fluctuation energy transfer between the cavity, mechanical and exciton mode is enhanced with an increase in the modulation frequency. Other parameters are also seen to influence the energy exchange. We study the entanglement dynamics between various modes of the system which is strongly related to the modulation frequency. Significant enhancement in entanglement is observed as we increase the modulation frequency. A transition from low stationary to large dynamical entanglement occurs as we switch on the modulation. This study opens up new possibilities for optimal control strategies and can be used for data signal transfer and storage in quantum communication platforms.

## I. INTRODUCTION

Theoretical studies and tremendous technological development over the last few decades have allowed a substantial degree of control over matter in a wide range of physical systems, ranging from electrons, photons, atoms to larger solid-state systems such as quantum dots and superconducting circuits. This has opened up the possibility of testing novel quantum mechanics and allowing us, among other things, to take major steps forward in investigating the quantum regime of macroscopic objects. In this context, the controlling of nano- and micromechanical oscillators at the quantum level is one of the key goals in today's quantum

research.

Quantum optomechanics [1–6] (i.e., the interaction of light radiation pressure with mechanical systems) comes as an effective and well-developed method for this. First, operation of the radiation pressure can be used to cool a (nano)micromechanical oscillator to its motional ground state[7]; this is a necessary step for quantum manipulation and could not be accomplished by direct means such as cryogenic cooling. Cooling has been experimentally demonstrated for a variety of physical implementations, including micromirrors in Fabry-Perot cavities [8, 9], microtoroidal cavities [10], or optomechanical crystals [11]. There is a close correlation between quantum optomechanics and nonlinear quantum optics, making it possible to model many (if not all) optomechanical effects based on well-known optical effects. As a result, optomechanics is a simple means of regulating the mechanical resonator at the quantum level.

In particular, Refs.[12–14] introduced an effective way of enhancing the generation of quantum effects, which relies on applying a periodic modulation to some of the system parameters (a similar result has also been found in the analogous context of nanoresonators and microwave cavities [15]).

The optomechanical coupling, which arises from the radiation pressure force exerted on the mirror by the cavity field, will result in the exchange of quantum states from one system to another. In an optomechanical system, the state of the cavity field can be coherently transferred, stored, and retrieved from the mirror[16, 17]. Here we demonstrate how one can actually achieve strong coupling between QD and a mirror in motional degrees of freedom. It results in a coherent exchange of average energy between them, in a steady-state [18, 19].

In the above scenario, we study the entanglement, which plays a crucial role in the field of quantum theory serving as a fundamental tool in the processing of quantum information, which is useful in quantum communication and computation tasks [21]. Entanglement has been observed between optical and mechanical resonator modes in a double-cavity system [22–25]. The purpose of entangled optomechanical systems [26, 27] is to create quantum communication networks where mechanical modes act as local nodes for the retrieval and storage of quantum information and optical modes for the transfer of information between these nodes [28–31]. Such hybrid systems are therefore useful in the fields of entanglement swapping [31], quantum teleportation [28, 30], and quantum telecloning [29]. The fast-growing field of cavity optomechanics [32–34] provides a better platform to prepare such an

entangled state in mechanical motion. In recent times, the research in this area has virtually exploded. Many studies have been reported on the entanglement generation between a cavity field and a mechanical oscillator [35–39] relying on the coupling of generic radiation-pressure. On the other hand, the modulation-assisted driving of a hybrid optomechanical device gives rise to interesting and rich entanglement dynamics which have been reported [40–42]. More recently, a study on enhanced entanglement is reported in which two-way coupled quantum dot inside the hybrid cavity system is introduced [43].

Recently, the experimental way of modulating the QD and modulating pump laser is studied [44–47]. A single QD coupled with a cavity can modulate the optical signal with very low control power since the system’s active volume is very low. The QD resonance is controlled via the Quantum Confined Stark Effect (QCSE) by electric signal. QD-resonance modulation controls laser transmission through the cavity. We use a lateral electric field to shift the QD resonance [45], thereby modulating the light [46].

In this paper, we analyze the dynamics of an optomechanical system which is periodically modulated. Although quantum optomechanics is now widely studied in a number of experimental setups, the modulation of the quantum dot (QD) frequency and amplitude of the pump laser that we are studying here is a very important feature that has not yet been implemented experimentally. We show the exchange of energy fluctuations between the various degrees of freedom of the hybrid system. We also see the effect of time-dependent detuning of QD on entanglement dynamics from which a new understanding of the entanglement process in quantum optomechanics can be established and finally, we also compare both modulating and non-modulating regimes. This study could make the path easy for further research in the field of quantum nonlinear optomechanics.

The organization of the paper is as follows. In section 2, we discuss the theory and model of the system and derive the quantum Langevin equations. In section 3, we follow the analytical technique and obtain the recursive relation to study the dynamics of the system. In the fourth section, we discuss the results and outcomes of the theory in which we discuss the dynamics of cavity modes, position and momentum quadrature of the mirror and their phase space trajectories. We also discuss the energy transfer between three modes of the system as well as dynamics of the average number of cavity photons, phonons and excitons. A detailed discussion about entanglement for our system is discussed in section four and conclusion in the last section.

## II. THEORY AND MODEL

In this article, the model considered is shown in Fig.1, where a single optical mode is interacting with a single mechanical mode in the presence of a QD whose frequency is modulated. The cavity is driven by an external pump laser as shown, whose amplitude is also modulated. The fabrication of the micro-cavity is done by DBR(Distributed Bragg Reflector). In this paper, the motivation of taking DBR based optomechanical system is to overcome two obstacles. The first one is to integrate two mirrors on a chip and the second is to involve a moving part within [48]. A typical solution is the use of DBRs for the fabrication of micro-cavities. One DBR is fixed and the other acts as the mechanical flexible part, as shown in Fig. 1. The confinement of light along the x-direction and the y-z plane is provided by DBR and air-guiding dielectric respectively. There are some known techniques by which the confinement of light along the longitudinal and transverse direction in the DBR can be achieved [49–53]. DBR mirror comprises of layers of the low and high refractive index of quarter-wavelength having AlGaAs as the first and last layer. The refractive index of AlGaAs is greater than that of air and lower than that of GaAs [54]. Hence, this structure results in a high-quality-factor semiconductor optical cavity. The total Hamiltonian for the system in the rotating frame of pump laser can be written as,

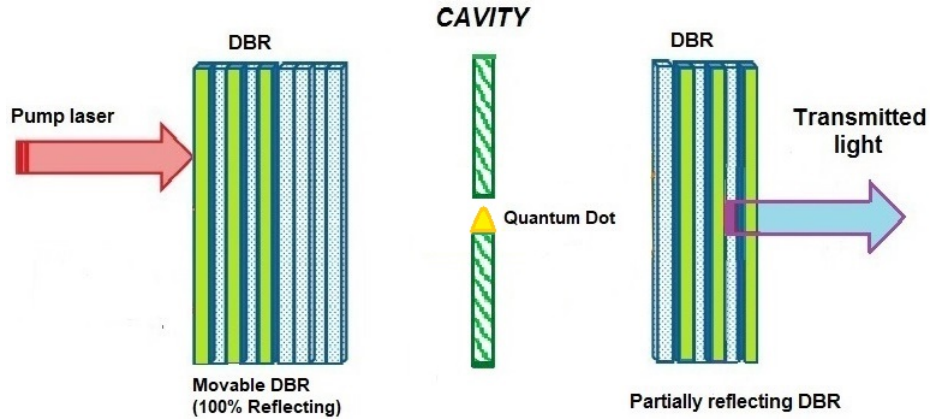


Figure 1: (Color online) Schematic display of the configuration discussed in the text. DBR mirrors with the cavity is shown in figure. The left side DBR is movable and quantum dot is placed in between the cavity. White and Green colored strips represent the GaAs and AlGaAs layers respectively.

$$\begin{aligned}\hat{H}' = & \hbar\Delta_c a^\dagger a + \frac{p^2}{2m} + \frac{1}{2}m\omega_m^2 q^2 + \hbar\Delta_d(t)\sigma_+\sigma_- - \hbar G a^\dagger a q + \hbar g_0(\sigma_+ a + \sigma_- a^\dagger) \\ & + i\hbar E(t)(a^\dagger - a)\end{aligned}\quad (1)$$

where;  $\Delta_c = \omega_c - \omega_L$ ,  $\Delta_d = \omega_d - \omega_L$ ,  $\Delta_d(t) = \frac{\Delta_0[1 - \cos(\omega_e t)]}{2}$  and  $E(t) = E_0 + \epsilon \cos(\Omega t)$ .

In the above Hamiltonian (eqn.1),  $a^\dagger(a)$  is the creation (annihilation) operator for the optical cavity field and the dimensionless momentum and position operators of the oscillator, defined by  $p$  and  $q$  respectively and these satisfy  $[q, p] = i\hbar$ . Also,  $\Delta_d(t)$  is the modulated detuning of the QD, where  $\Delta_0$  is the maximum detuning of the QD resonance (this is proportional to the amplitude of the electrical signal applied to tune the QD) and  $\omega_e$  is the frequency of the modulating electrical signal. Also  $G$  and  $g_0$  is the optomechanical coupling constant and coupling between the optical cavity and quantum dot respectively. Here,  $E(t)$  is external drive intensity having frequency  $\Omega$ ,  $E_0$  is the constant driving amplitude that takes the real value and  $\epsilon$  is the amplitude of the modulation. For simplicity, we assume  $\Omega = \omega_e$ .

To study the dynamics of the given system, we write the quantum Langevin equations for the Hamiltonian (eqn. 1) as,

$$\dot{a} = -i\Delta_c a - \kappa_a a + iGa q + E(t) - ig_0\sigma_- + \sqrt{2\kappa_a}a^{in}, \quad (2)$$

$$\dot{p} = -\omega_m q + Ga^\dagger a - \gamma p + \zeta(t), \quad (3)$$

$$\dot{q} = \omega_m p, \quad (4)$$

$$\dot{\sigma}_- = i\Delta_d(t)\sigma_z\sigma_- + ig_0 a\sigma_z - \kappa_d\sigma_-. \quad (5)$$

Here  $\gamma$  and  $\kappa_a$  are the mechanical and optical damping rates, respectively. Radiation vacuum input noise is represented by  $a^{in}$  obeying the standard correlation relation  $\langle a^{in\dagger}(t)a^{in}(t) + a^{in}(t')a^{in\dagger}(t') \rangle = \delta(t - t')$  and  $\frac{1}{2} \langle \zeta(t)\zeta(t') + \zeta(t')\zeta(t) \rangle = \gamma(2n_b + 1)\delta(t - t')$  denotes the Brownian noise operator. Here,  $n_b = 1/\exp(\hbar\omega/k_B T - 1)$  is the mean phonon number of the mechanical bath which gauges the temperature  $T$  of the system [55–57].

To solve equation(2)-(5), we use mean-field approximation to express relevant operators as sum of the mean values (large) and fluctuation terms (small).

i.e.,  $o = O + \delta o = (o = q, p, a, \sigma)$  In this way we can write Heisenberg equation for mean values  $O$ , in the form of a set of classical nonlinear differential equations

$$\dot{Q} = \omega_m P, \quad (6)$$

$$\dot{P} = -\omega_m Q + G|A|^2 - \gamma P, \quad (7)$$

$$\dot{A} = (-i\Delta_c - \kappa_a)A + iGAQ + (E_0 + \epsilon \cos(\Omega t)) - ig_0\sigma_-, \quad (8)$$

$$\dot{\sigma}_- = -(\kappa_d - i\frac{\Delta_0}{2}[1 - \cos(\omega_e t)]\sigma_- + ig_0A\sigma_z, \quad (9)$$

and a set of quantum linear differential equation for the fluctuations-

$$\dot{\delta q} = \omega_m \delta p, \quad (10)$$

$$\dot{\delta p} = -\omega_m \delta q + G(A\delta a^\dagger + A^\dagger \delta a) - \gamma \delta p + \zeta(t), \quad (11)$$

$$\dot{\delta a} = (-i\Delta_c - \kappa_a)\delta a + iG(A\delta q + Q\delta a) + \sqrt{2k_a}a_{in} - ig_0\delta\sigma_-, \quad (12)$$

$$\dot{\delta\sigma}_- = -(\kappa_d - i\frac{\Delta_0}{2}[1 - \cos(\omega_e t)]\sigma_- + ig_0\delta a\sigma_z, \quad (13)$$

### III. DYNAMICAL BEHAVIOR OF THE SYSTEM

In the following sections, we now study the dynamics of the system based on the eqns. (6)-(13). Equation (6)-(9), are nonlinear and can be solved numerically. We assume that we are distant from optomechanical instability and multistabilities. Taking the perturbation on optomechanical coupling, and since  $E(t + \tau) = E(t)$ , one finds that the mean values are moving towards the asymptotic periodic orbit with the same  $2\pi/\Omega$  periodicity.

Thus, this justifies performing a double expansion of the asymptotic solution  $< O(t) (O = q, p, a, \sigma)$  in the power of coupling constant  $G_0$  and also in terms of fourier components:

$$< O(t) > = \sum_{j=0}^{\infty} \sum_{n=-\infty}^{\infty} O_{n,j} e^{in\Omega t} G^j, \quad (14)$$

where,  $\Omega = 2\pi/\tau$  is the frequency of the modulation.

Now, substitute equation (14) in Eqn. (6-9) and also note similar fourier series of the periodic driving amplitude  $E(t)$ . This yields,

$$< O(t) > = \sum_{n=-\infty}^{\infty} E_n e^{in\Omega t}, \quad (15)$$

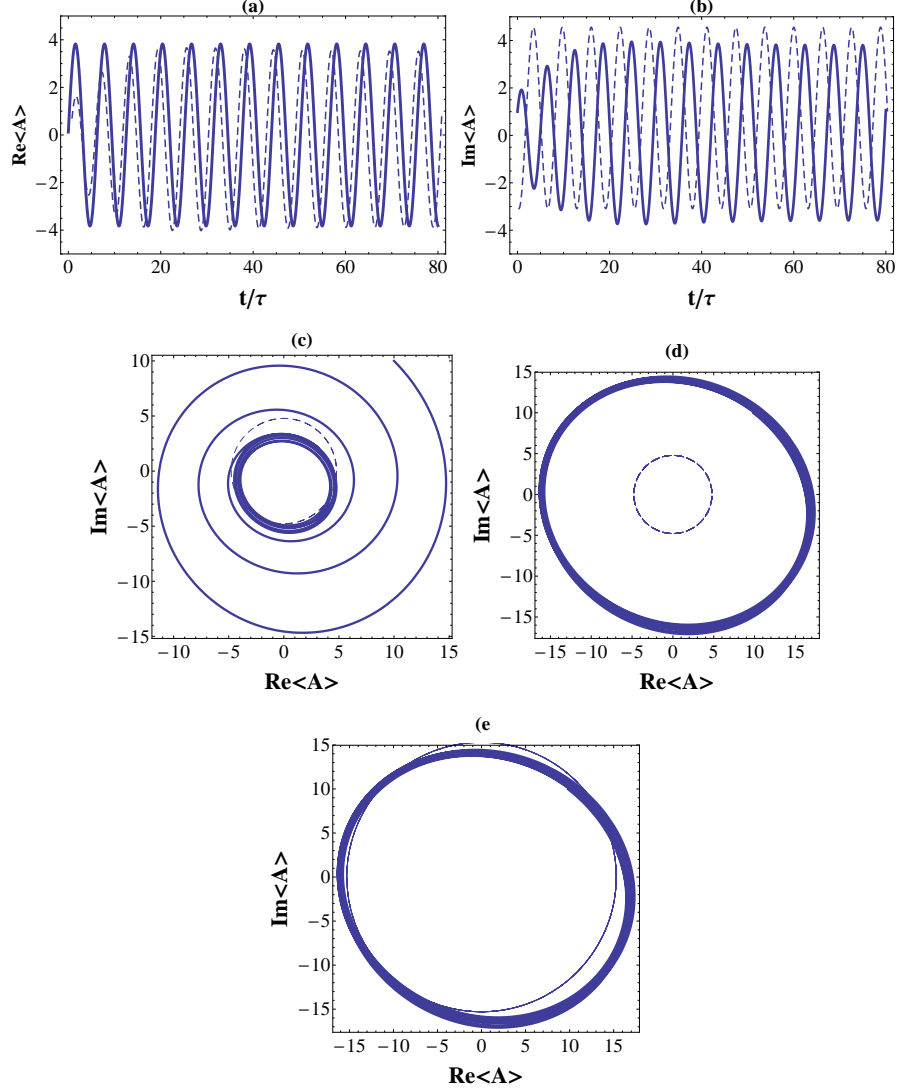


Figure 2: (Color online): (a), (b)- Time evolution of the real and imaginary parts of the cavity mode mean value  $\text{Re}\langle a(t) \rangle$  and  $\text{Im}\langle a \rangle$  respectively. (c)- The phase space trajectories of cavity modes  $\langle a(t) \rangle$ . Numerical simulation for  $t = [0, 20 \tau]$  (Thick line) and analytical approximation (Thin-dotted line). For (d)-  $t = [25, 35 \tau]$  (e)-  $t = [35, 50 \tau]$ . The chosen parameters in units of  $\omega_m$  are:  $g_0=0.3$ ,  $N=1$ ,  $G=0.01$ ,  $\gamma=0.01$ ,  $E_0=1$ ,  $E_1 = E_{-1} = 10$  (b), 32 (e), 10 (d), 32 (e),  $\kappa_a=0.1$ ,  $\epsilon=1$  (a, b), 4 (c, d, e),  $\Delta_0=1$ ,  $\kappa_d=0.2$ ,  $\Omega=1$ ,  $\Delta_c=1$ .

and

$$\langle O(t) \rangle = \sum_{n=-\infty}^{\infty} \Delta_0 e^{in\Omega t}. \quad (16)$$

One finds that the coefficients  $O_{n,j}$  (time independent) can be calculated by the following recursive relations:-

$$\begin{aligned}
p_{n,0} = 0, q_{n,0} = 0, a_{n,0} &= \frac{E_{-n}(in\Omega\kappa_d)}{[(\kappa_a + i(\Delta_c + n\Omega))(in\Omega + \kappa_d) - g_0^2 N]}, \\
\sigma_{n,0} &= \frac{E_{-n}(ig_0 N)}{[(\kappa_a + i(\Delta_c + n\Omega))(in\Omega + \kappa_d) - g_0^2 N]},
\end{aligned} \tag{17}$$

associated with zeroth order perturbation with respect to  $G$  and for all  $j \geq 1$  we have

$$p_{n,j} = \frac{in\Omega q_{n,j}}{\omega_m}, q_{n,j} = \omega_m \sum_{k=0}^{j-1} \sum_{m=-\infty}^{\infty} \frac{a_{m,k}^\dagger a_{n+m,j-k-1}}{[\omega_m^2 - (n\Omega)^2 + i\gamma n\Omega]} \tag{18}$$

$$a_{n,j} = i \sum_{k=0}^{j-1} \sum_{m=-\infty}^{\infty} \frac{a_{m,k} q_{n-m,j-k-1} ([\kappa_a + i(\Delta_c + n\Omega)][i(n\Omega - \Delta_0) + \kappa_a])}{([\kappa_a + i(\Delta_c + n\Omega)][i(n\Omega - \Delta_0) + \kappa_d] - g_0^2 N)}, \tag{19}$$

$$\sigma_{n,j} = -g_0 N \sum_{k=0}^{j-1} \sum_{m=-\infty}^{\infty} \frac{a_{m,k} q_{n-m,j-k-1} ([\kappa_a + i(\Delta_c + n\Omega)])}{([\kappa_a + i(\Delta_c + n\Omega)][i(n\Omega - \Delta_0) + \kappa_d] - g_0^2 N)}. \tag{20}$$

In all the above calculations, we truncated the series in the last equation to the terms with subscripts  $|n| \leq 1$  and  $j \leq 2$ .

Once we have obtained the dynamics of the mean values, now the dynamics of the quantum fluctuations can be solved. To proceed further, in equation (10-13), we ignore the second and higher order small terms and write the field operators in quadrature form as  $\delta x = \frac{1}{\sqrt{2}} (\delta a^\dagger + \delta a)$ ,  $\delta y = \frac{1}{\sqrt{2}i} (\delta a^\dagger - \delta a)$ ,  $\delta v = \frac{1}{\sqrt{2}} (\delta \sigma_-^\dagger + \delta \sigma_-)$ ,  $\delta w = \frac{1}{\sqrt{2}i} (\delta \sigma_-^\dagger - \delta \sigma_-)$  and the noise  $\delta x^{in} = \frac{1}{\sqrt{2}} (\delta a^{in\dagger} + \delta a^{in})$ ,  $\delta y^{in} = \frac{1}{\sqrt{2}i} (\delta a^{in\dagger} - \delta a^{in})$ ,

The quantum Langevin equations for these quadrature fluctuations can be written in a matrix form:

$$\dot{u} = Du + k, \tag{21}$$

where,  $u = (\delta q, \delta p, \delta x, \delta y, \delta u, \delta v)^T$  is the fluctuation vector,  $k = (0, \zeta, \kappa_a, \kappa_d, 0, 0)^T$  is the noise vector and the time dependent matrix is given by:

$$D = \begin{bmatrix}
0 & \omega_m & 0 & 0 & 0 & 0 \\
-\omega_m & -\gamma_m & \sqrt{2}G\text{Re}(A) & \sqrt{2}G\text{Im}(A) & 0 & 0 \\
-\sqrt{2}G\text{Im}(A) & 0 & -\kappa_a & F_1 & 0 & g_0 \\
\sqrt{2}G_1\text{Re}(A) & 0 & -F_1 & -\kappa_a & -g_0 & 0 \\
0 & 0 & 0 & -g_0 N & -\kappa_d & -MN \\
0 & 0 & g_0 N & 0 & MN & -\kappa_d
\end{bmatrix},$$



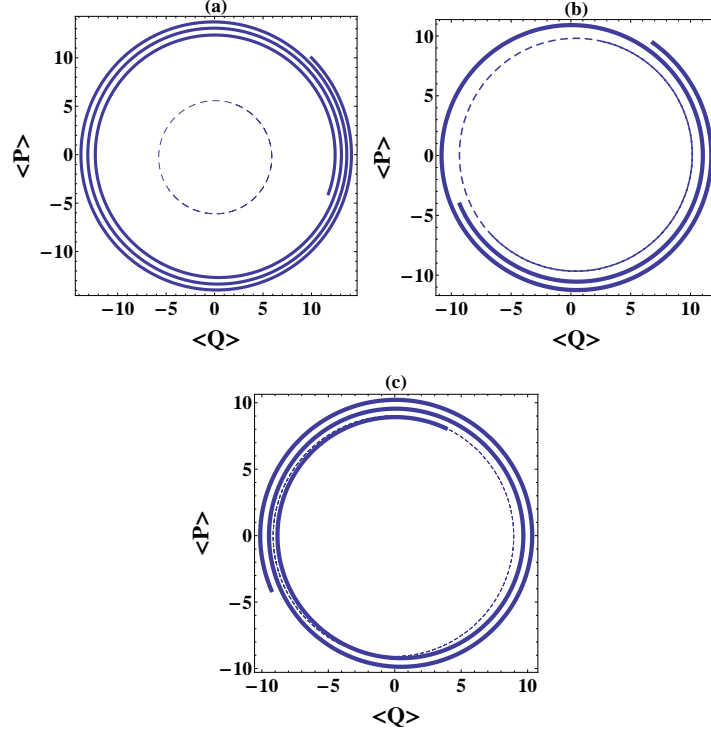


Figure 3: (Color online) Phase space trajectories of dimensionless mechanical position and momentum mean values  $\langle Q(t) \rangle$  and  $\langle P(t) \rangle$  respectively. Numerical simulation for  $t = [0, 20\tau]$  (Thick line) and analytical approximation (Thin-dotted line). For (b)-  $t = [25, 35\tau]$  (c)-  $t = [35, 50\tau]$ . All the chosen parameters are identical to those in Fig.2.

with

$$F_1 = (\Delta_c - GQ),$$

$$M = \frac{\Delta_0}{2} (1 - \cos(\omega_e t)), \quad (22)$$

and  $N = \langle \sigma_z \rangle$  is the difference of population in the ground state and excited state of Q.D [58, 59].

Equation(21) is stochastic and needs some manipulation. Nonetheless, since we have linearized the dynamics and the noise terms are Gaussian zero-mean, fluctuations in the stable regime will also develop into asymptotic Gaussian zero-mean state. Instead, the correlation matrix  $V$  of elements completely defines the state of the system.

$$V_{ij} = \frac{1}{2} \langle u_i(t)u_j(t) + u_j(t)u_i(t) \rangle, \quad (23)$$

and attain its dynamic equation:-

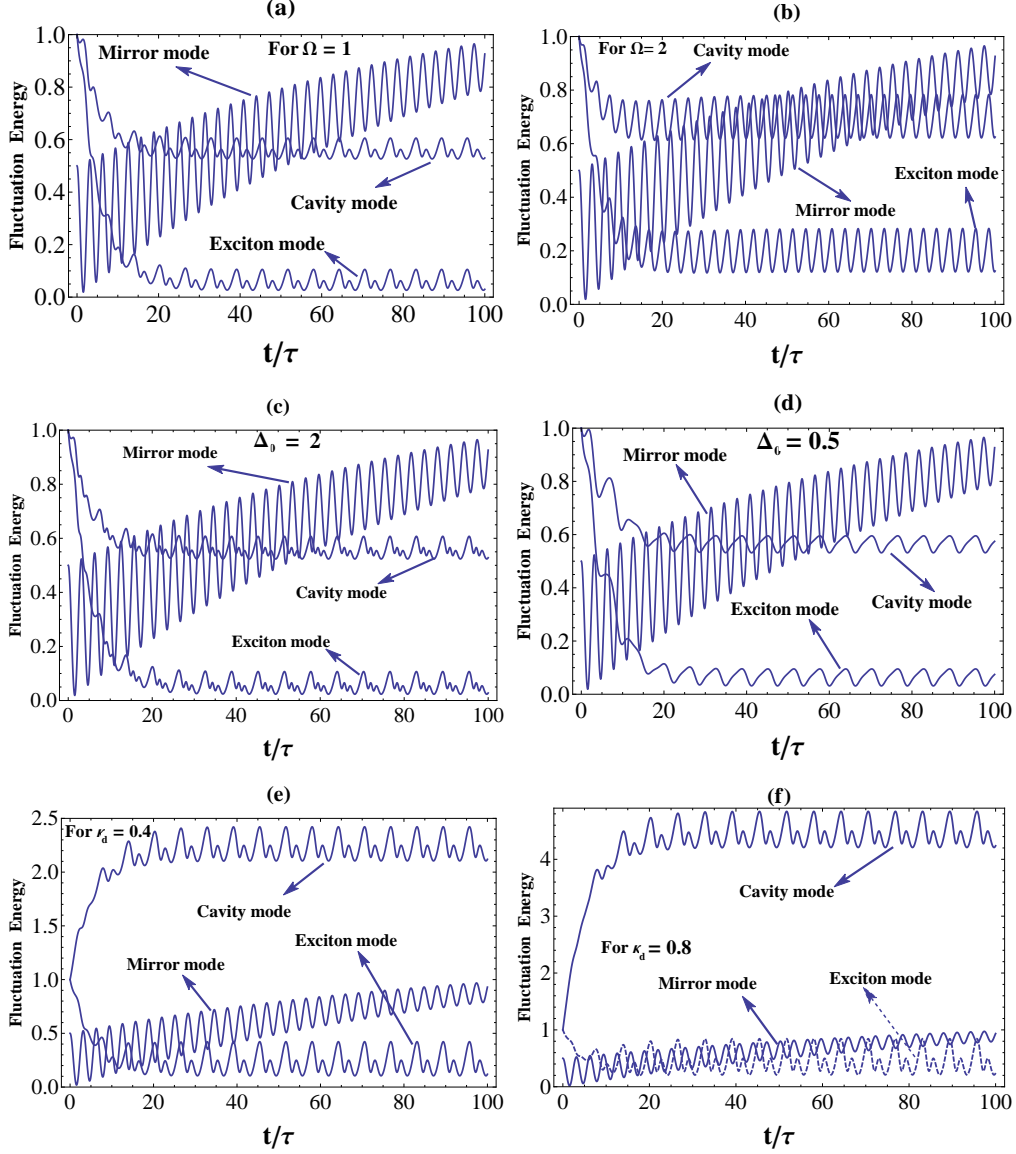


Figure 4: (Color online) Energy fluctuation transfer between different modes of the system. The chosen parameters in units of  $\omega_m$  are:  $\kappa_a=0.1$ ,  $E_0=1$ ,  $\epsilon=1$ ,  $\Delta_0=1$ ,  $\kappa_d=0.1$ ,  $\Delta_c=1$ ,  $g_0=1$ ,  $G=0.005$ ,  $N=1$ ,  $\Omega=1$ ,  $\gamma_m=0.01$ .

$$\dot{V} = DV + VD^T + N, \quad (24)$$

where  $D^T$  is transpose of  $D$ , and  $K$  is the diagonal noise correlation matrix with diagonal elements  $(0, \gamma(2n_b + 1), \kappa_a, \kappa_a, 0, \gamma(2n_b + 1), \kappa_d, \kappa_d)$ .

Now, equation(24) is an ordinary linear differential equation which gives 36 equations in terms of  $V_{ij}$ . We can solve it numerically to study the dynamical behavior of the system.

#### IV. RESULTS AND DISCUSSION

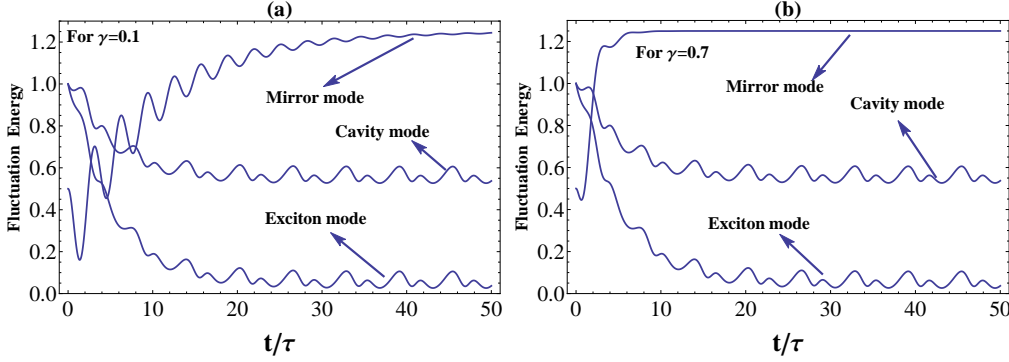


Figure 5: (Color online) Energy fluctuation transfer between different modes of the system; (a)- For  $\gamma=0.1$ . (b)- For  $\gamma=0.7$ . The chosen parameters in units of  $\omega_m$  are:  $\kappa_a=0.1$ ,  $E_0=1$ ,  $\epsilon=1$ ,  $\Delta_0=1$ ,  $\kappa_d=0.1$ ,  $\Omega=1$ ,  $\Delta_c=1$ ,  $g_0=1$ ,  $G=0.005$ .

By approximating the asymptotic classical mean values in equations (18-20), we truncate the series only to the first few terms with indexes  $j=0,1,2$  and  $|n| \leq 1$  which gives rise to a good approximation. All frequencies are dimensionless w.r.t  $\omega_m$ .

In fig.2(a) and (b), we plot the time evolution of the real and imaginary parts of the cavity mode mean value  $\text{Re}\langle a(t) \rangle$  and  $\text{Im}\langle a(t) \rangle$  respectively. We find that in long time limit  $\langle a(t) \rangle$  is indeed  $\tau(=2\pi/\Omega)$  periodicity and that the numerical(thick line) and analytical results(thin-dotted line) are in good agreement.

To gain more insight about the dynamics, we plot the phase-space trajectory of cavity mode and mirror mode from  $t=0$  to  $t=50\tau$ . Fig.2(c), shows that for less than 50 modulation period, the first moment reaches quasi-periodic orbit which is approximated by analytical results(thin-dotted line). In fig.2(d) and 2(e), we see that for lower mechanical damping rate  $\gamma \ll \kappa_a$ , it takes longer time for the phase space trajectories of the cavity mean values to approach the limit cycle given by the analytical solution from equation(19),(thin-dotted line).

In fig.3, we study the phase space quadrature of the mechanical oscillator. We notice that for  $\gamma \ll \kappa_a$ , it takes a longer time for the phase space trajectories of the mechanical oscillator of the mirror to approach the limit cycle given by the analytical solution from (18),(thin-dotted line).

To study the fluctuation energy transfer between different modes, we can employ a suit-

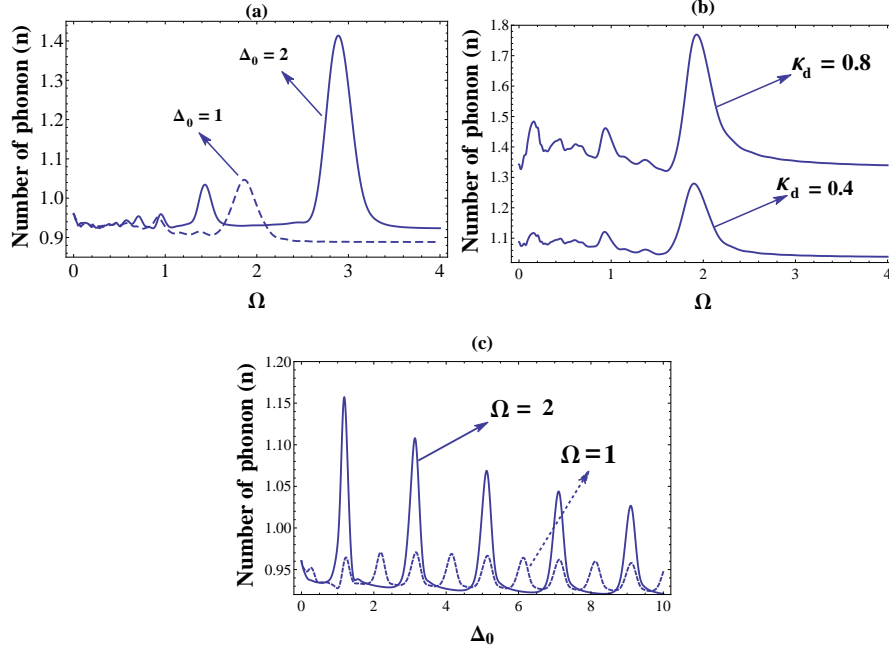


Figure 6: (Color online) (a): Average Number of phonons as a function of  $\Omega$  for different value of  $\Delta_0$ . (b): Avg. No. of phonons as a function of  $\Omega$  for different value of  $\kappa_d$ . (c): Avg. No. of phonons as a function of  $\Delta_0$  for different value of  $\Omega$ . The chosen parameters in units of  $\omega_m$  are:  $\kappa_a=0.1$ ,  $E_0=1$ ,  $\epsilon=1$ ,  $\kappa_d=0.2$ ,  $\Delta_c=1$ ,  $g_0=0.4$ ,  $N=1$ ,  $G=0.1$ ,  $\Omega=1$ ,  $\gamma=0.005$ .

able pulse shape  $E(t)$  that would simultaneously couple the cavity mode to fluctuations of the exciton and the mirror. This would allow us to transfer the fluctuation energy from the mirror to the exciton via the cavity mode and vice versa, in a controlled and deterministic way for long times. The fluctuation energy for cavity mode, mirror mode and exciton are given by  $\langle \delta a^\dagger \delta a \rangle$ ,  $\langle \delta q^2 \rangle$  and  $\langle \delta \sigma^\dagger \delta \sigma \rangle$  respectively. So, using equation (24) we can write approximately;  $\langle \delta a^\dagger \delta a \rangle \simeq \frac{\langle \delta x^2 + \delta y^2 \rangle}{2} = \left( \frac{V_{33} + V_{44}}{2} \right)$ ,  $\langle \delta q^2 \rangle = V_{11}$  and  $\langle \delta \sigma^\dagger \delta \sigma \rangle = \left( \frac{V_{55} + V_{66}}{2} \right)$ . Unlike in stimulated Raman adiabatic passage (STIRAP) [60], in this case, the intermediary cavity mode would be populated and so the pulse duration should be well within the decay timescale of the cavity mode. Note that such a method of energy transfer is not truly adiabatic, because it involves exchange of energy between various adiabatic states. In Fig. 4, we show how the fluctuation energies (dimensionless w.r.t  $\omega_m$ ) can be transferred between exciton, mirror and cavity mode. We see in fig. 4(a) and 4(b), that fluctuation energy transfer between cavity and mirror mode becomes more enhanced with increase in the modulation frequency. In fig. 4(c) and 4(d), we notice that the energy transfer between the mechanical mode and exciton mode diminishes as QD decay rate  $\kappa_d$  increases. On the

other hand we notice that the cavity mode gains energy when  $\kappa_d$  increases. In fig. 4(e) and 4(f), as the laser frequency shift towards cavity resonance frequency the energy transfer takes place between mirror mode and cavity mode more prominently.

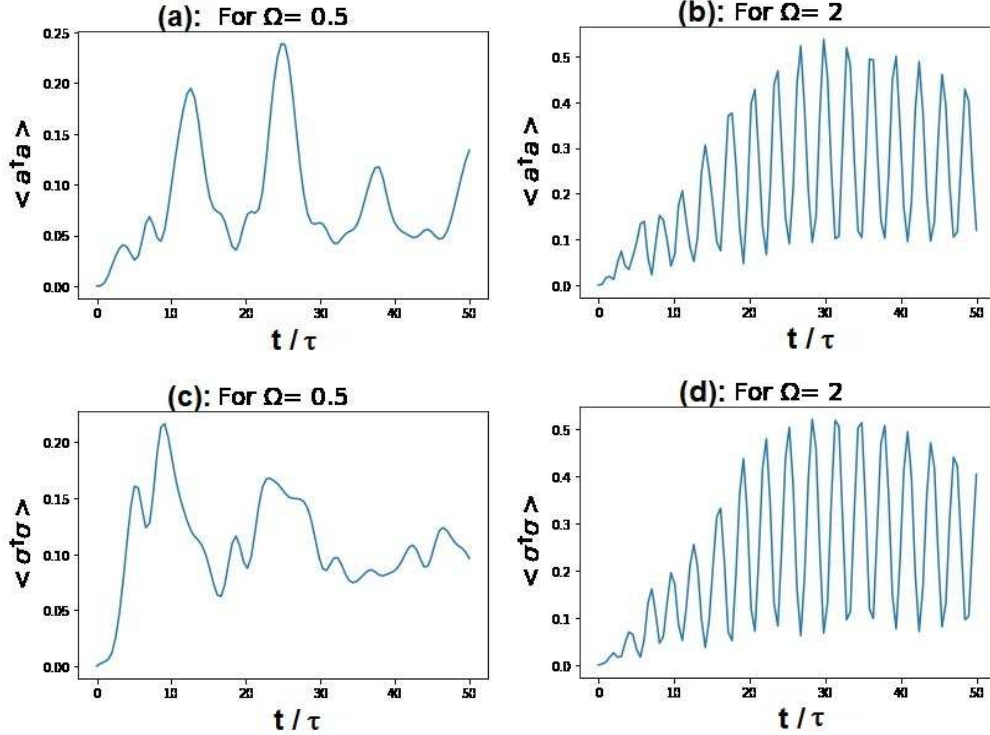


Figure 7: (Color online) Average value of photon w.r.t time. (a)- For  $\Omega=0.5$ , (b)- for  $\Omega=2$ , and average value of exciton (c)- for  $\Omega=0.5$ , (d)- for  $\Omega=2$ . The chosen parameters in units of  $\omega_m$  are:  $\kappa_a=0.1$ ,  $E_0=1$ ,  $\epsilon=1$ ,  $\Delta_0=1$ ,  $\kappa_d=0.1$ ,  $\Delta_c=1$ ,  $g_0=1$ ,  $G=0.005$ ,  $N=1$ ,  $\gamma=0.1$ .

In fig. 5, we plot fluctuation energy for two different values of mirror decay rate ( $\gamma$ ). We observe that as the decay rate for the mirror increases, the energy gained by the mirror mode increases rapidly with time. i.e., the mirror attains the maximum energy at a much shorter time for large  $\gamma$ .

As already mentioned, thanks to Gaussianity of the asymptotic solution, all relevant information about the system can be extracted directly from the correlation matrix  $V$ . In particular, we will focus on the following quantity: the average number of phonons in the mirror.

The number of phonons 'n', as we know depends on position and momentum of the moving mirror and this can be expressed using the approximate relation [61],

$$\hbar\omega_m \left( n + \frac{1}{2} \right) \approx \left( \frac{\hbar\omega_m}{2} \right) < \delta q^2 + \delta p^2 > = \left( \frac{\hbar\omega_m}{2} \right) (V_{11} + V_{22}), \quad (25)$$

which holds if the modulation of the external pump frequency is not too strong. This tells how far the system is from the ground state.

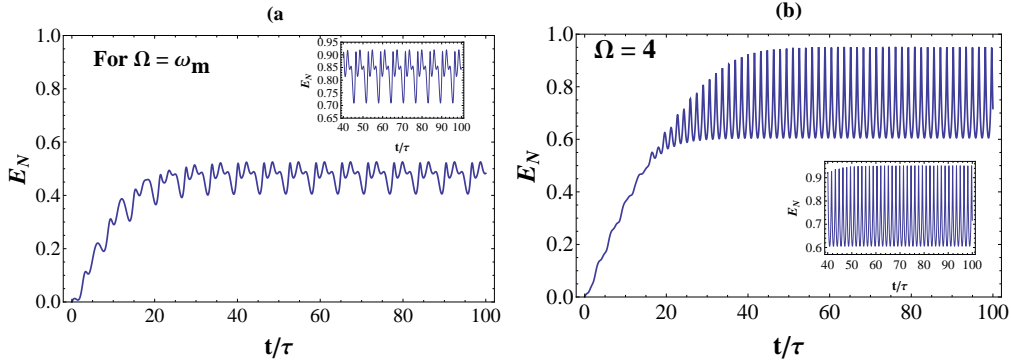


Figure 8: (Color online) Dynamics of the QD- mirror entanglement  $(E_N)_{md}$  as a function of time for different modulation regime: (a).  $\Omega = \omega_m$ , (b).  $\Omega = 4\omega_m$ ; The chosen parameters in units of  $\omega_m$  are:  $\kappa_a=0.1$ ,  $\kappa_d=0.2$ ,  $\Delta_0=1$ ,  $\Delta_c=1$ ,  $g_0=0.3$ ,  $G=0.005$ ,  $N=1$ ,  $n_b = 0$ ,  $\gamma=0.01$ ,  $\epsilon=0.5$ ,  $E_0 = 1$ .

In fig. 6(a), we study the behavior of average number of phonons w.r.t modulation frequency ( $\Omega$ ) for two different values of QD detuning( $\Delta_0$ ). As we scan across  $\Omega$ , multiple peaks appear with increasing height as  $\Omega$  increases. At  $\Delta_0$ , the highest peak appears at around  $\Omega=1.8$  with  $n=1$ . For  $\Delta_0=2$ , two prominent peaks are visible at  $\Omega=1.3$  with  $n=1.0$  and  $\Omega=3$  with  $n=1.4$ . This indicates that as  $\Delta_0$  increases, the number of resonant interactions that transfer energy to the mechanical mode increases. In fig. 6(b), as the decay rate of the QD ( $\kappa_d$ ) increase, we see the number of phonon also increases which indicates that a rapidly decaying QD transfers higher energy to the mechanical mode. In fig. 6(c), we plot the number of phonon w.r.t QD detuning ( $\Delta_0$ ) for two different value of the pump modulation frequency ( $\Omega$ ). We see that a higher  $\Omega$  is able to transfer more energy to the mechanical mode which is also visible in fig. 6(a).

Fig. 7(a) and 7(b) shows the time dynamics of the average number of photons ( $a^\dagger a$ ) and fig. 7(c) and 7(d) displays the time dynamics of number of excitons ( $\sigma^\dagger \sigma$ ). On increasing the pump modulation frequency  $\Omega$ , we observe a rapid variation in  $\langle a^\dagger a \rangle$  and  $\langle \sigma^\dagger \sigma \rangle$  accompanied by an increase in the number of photons and excitons. We can thus refer from figs. (6) and (8) that as the pump modulation frequency  $\Omega$  increases, an enhanced transfer of energy to the mechanical, optical and excitation mode is visible.

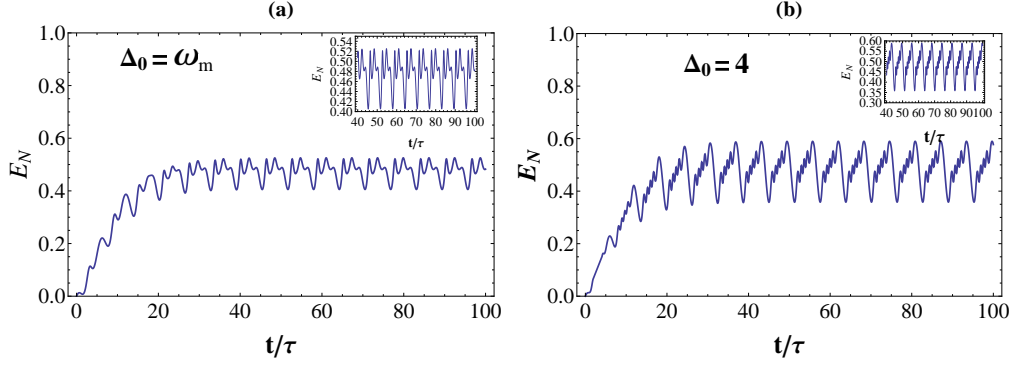


Figure 9: (Color online) Dynamics of the QD- mirror entanglement  $(E_N)_{md}$  as a function of time for QD detuning values: (a).  $\Delta_0 = \omega_m$ , (b).  $\Omega = \omega_m$ ; The chosen parameters in units of  $\omega_m$  are:  $\kappa_a=0.1$ ,  $\kappa_d=0.2$ ,  $\Delta_0=1$ ,  $\Delta_c=1$ ,  $g_0=0.3$ ,  $G=0.005$ ,  $n_b = 0$ ,  $N=1$ ,  $\gamma=0.01$ ,  $\epsilon=0.5$ ,  $E_0 = 1$ .

## V. ENTANGLEMENT

Entanglement [62], a basic phenomenon of quantum mechanics, has been considered to be a primary tool for quantum computing, information processing and quantum communication [63–67]. Many physical system have been prepared and manipulated so far, to study quantum entanglement, such as individual atoms [68], photons [69, 70], ions [71] between optical photon and solid-state spin qubit [72], etc. Entanglement has also been observed in an optomechanical system consisting of a quantum well embedded inside [73]. To study the entanglement there are different methods, but Logarithmic negativity is one of the commonly used methods [74].

Equation (24) is a first order inhomogeneous differential equation which contains 36 elements and these could be numerically solved with initial condition,  $V(0)=\text{Diag}[n_{th}+1/2, n_{th}+1/2, 1/2, 1/2, 1/2, 1/2]$ . In our study, we have assumed that a mechanical oscillator is prepared in its thermal state at the temperature  $T$  and cavity field in its vacuum state.

In order to proceed with the numerical investigation of mechanical entanglement, we first define the exact form of time modulation for both the external driving and the quantum dot cavity coupling strength.  $E(t) = E_0 + \epsilon \cos(\Omega t)$  and  $\Delta_0(t) = \frac{\Delta_0}{2} (1 + \cos(\Omega t))$ .

In fig. 8, we plot the time evolution of the QD-mirror entanglement  $(E_N)$  (see appendix A) for different values of  $\Omega$ . It is observed that for the value of modulation frequency ( $\Omega=\omega_m$ ), the system attains a small average entanglement of 0.45 (see fig. 8(a)) compared

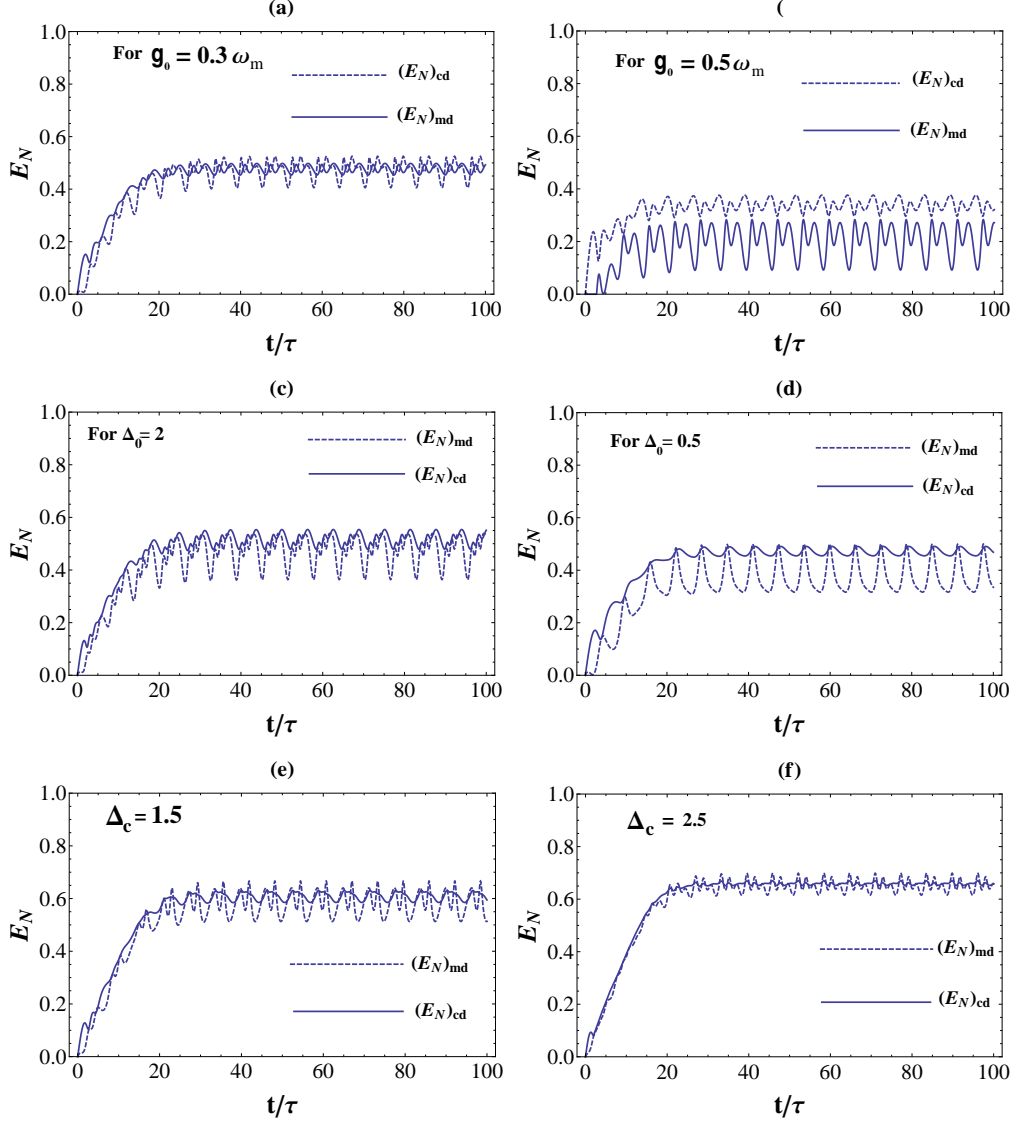


Figure 10: (Color online) Dynamics of the QD- mirror entanglement and QD-cavity entanglement  $(E_N)_{md}$  and  $(E_N)_{cd}$  respectively as a function of time. The chosen parameters in units of  $\omega_m$  are:  $\kappa_a=0.1$ ,  $\kappa_d=0.2$ ,  $\Delta_0=1$ ,  $\Delta_c=1$ ,  $g_0=0.3$ ,  $G=0.005$ ,  $n_b = 0$ ,  $\gamma=0.01$ ,  $N=1$ ,  $\epsilon=0.5$ ,  $E_0 = 1$ .

to that for  $\Omega=4\omega_m$  (see fig. 8(b)). We notice that as we increase the modulation frequency, initially there is a significant enhancement in entanglement ( $E_N$ ) and then tends to an average steady-state value. This enhancement becomes more profound as we increase the modulation frequency ( $\Omega$ ). Moreover, in large time limit, we note that entanglement acquires fast periodic modulation around a steady value as we increase the modulation frequency (see plot, 8(a) and 8(b)).

The average steady value for  $\Omega=4\omega_m$  is significantly higher ( $=0.8$ ) compared to that



for  $\Omega=\omega_m$  ( $=0.45$ ). The maximum entanglement attained for  $\Omega=\omega_m$  is  $E_N=0.52$  while for  $\Omega=4\omega_m$  it is  $E_N=0.95$ . For  $\Omega=4\omega_m$ , the amplitude of oscillations are also much larger compared to that for  $\Omega=\omega_m$ .

In fig. (9), we once again depict the time evolution of QD-mirror entanglement ( $E_N$ ) for different QD detuning ( $\Delta_0$ ). For  $\Delta_0=\omega_m$ , the maximum entanglement obtained is 0.51 while for  $\Delta_0=4\omega_m$ , the maximum entanglement attained is 0.60. The amplitude of oscillations for  $\Delta_0=4\omega_m$  is much higher compared to that for  $\Delta_0=\omega_m$ .

These mentioned behaviour shows that modulating pump frequency ( $\Omega$ ) and QD detuning ( $\Delta_0$ ) playing a significant role and one can control the entanglement by appropriately tuning these parameters.

In fig.10, we have shown the behavior of mirror-dot entanglement ( $(E_N)_{md}$ ) and cavity-dot entanglement ( $(E_N)_{cd}$ ) for various combination of parameters. In fig. 10(a) and (b), we note that as the coupling between cavity and QD increase the difference of both the entanglement increase and for higher value of coupling constant  $g_0$  both entanglement decreases as compared to lower value of  $g_0$  while the cavity-dot entanglement ( $(E_N)_{cd}$ ) attains higher value as compared to mirror-dot entanglement ( $(E_N)_{md}$ ). In fig. 10(c) and (d), as the value of QD detuning ( $\Delta_0$ ) decrease, the amplitude of both the entanglement slows down as compared to higher value of ( $\Delta_0$ ). In fig. 10(e) and (f), we note that as the value of cavity detuning ( $\Delta_c$ ) increase, the amplitude difference between the two entanglement tends to decrease.

This behavior shows that mirror-dot entanglement ( $(E_N)_{md}$ ) and cavity-dot entanglement ( $(E_N)_{cd}$ ) can be effectively controlled by appropriate changes to the QD-cavity coupling ( $g_0$ ), QD detuning ( $\Delta_0$ ) and cavity detuning ( $\Delta_c$ ).

In fig.11, we study the dynamics of the QD-cavity entanglement  $(E_N)_{cd}$  as a function of time for different values of QD decay rate ( $\kappa_d$ ). It is obvious from the fig. 11 that a fast decaying QD generates less entanglement. We note that both  $(E_N)_{cd}$  and  $(E_N)_{md}$  show decreasing behavior between  $\Delta_c=0$  to  $\Delta_c=-2$ . In particular in this  $\Delta_c$  window  $(E_N)_{md}$  completely vanishes.

Fig.(12) shows the plot of QD- mirror entanglement  $(E_N)_{md}$  and QD-cavity entanglement  $(E_N)_{cd}$  as a function of cavity detuning ( $\Delta_c$ ). However both the values of entanglement approach the same value as the detuning increases towards large positive values.

In fig.(13), we plot  $(E_N)_{md}$  for two regimes: with and without modulation. Interestingly

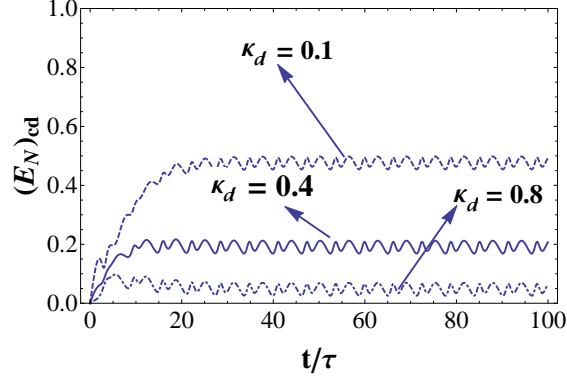


Figure 11: (Color online) Dynamics of the QD-cavity entanglement  $(E_N)_{cd}$  as a function of time for different values of QD decay rate ( $\kappa_d$ ). The chosen parameters in units of  $\omega_m$  are:  $\kappa_a=0.1$ ,  $\Delta_0=1$ ,  $\Delta_c=1$ ,  $g_0=0.3$ ,  $G=0.005$ ,  $n_b = 0$ ,  $\gamma=0.01$ ,  $N=1$ ,  $\epsilon=0.5$ ,  $E_0= 1$ .

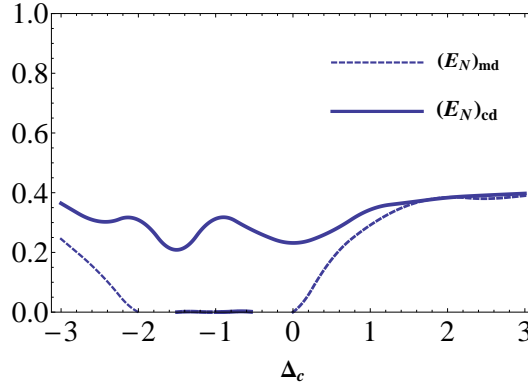


Figure 12: (Color online) Dynamics of the QD- mirror entanglement  $(E_N)_{md}$  and QD-cavity entanglement  $(E_N)_{cd}$  as a function of cavity detuning ( $\Delta_c$ ). The chosen parameters in units of  $\omega_m$  are:  $\kappa_a=0.1$ ,  $\kappa_d=0.2$ ,  $\Delta_0=1$ ,  $\Delta_c=1$ ,  $g_0=0.3$ ,  $G=0.005$ ,  $\Omega=1$ ,  $n_b = 0$ ,  $\gamma=0.01$ ,  $N=1$ ,  $\epsilon=0.5$ ,  $E_0= 1$ .

the modulation generates a large amount of entanglement compared to the non-modulating case. This can be explained by the fact that as noted previously, modulation enhances the energy transfer between various modes.

## VI. CONCLUSION

In this paper, we have analyzed the dynamical behavior of a hybrid optomechanical device containing a single quantum dot whose frequency and the amplitude of the external pump is modulated. The dynamics of the system for mean value of position, momentum and cavity photon number is discussed analytically and verified numerically. The fluctuation energy

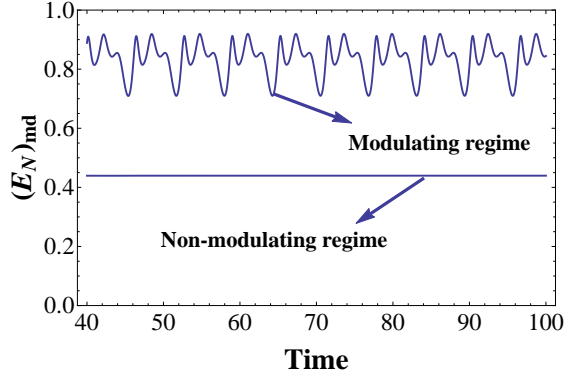


Figure 13: (Color online) Dynamics of the QD- mirror entanglement  $(E_N)_{md}$  as a function of time (a):- Modulation regime (b):- Non modulating regime. All the parameters are same as fig.(12).

transfer between cavity mode, mirror mode and exciton is studied. The system parameters are seen to influence the fluctuation energy transfer between these three modes. As we increase the modulation frequency energy exchange between the cavity and mirror mode is enhanced. Further, the different physical parameters of the system are observed to influence the average number of phonons, photons and excitons and give some interesting results such as a rapidly decaying exciton mode and higher modulation frequency is able to transfer more energy to the mechanical mode. We have shown that the modulation also controls the entanglement for appropriate system parameters. Interestingly, we find that modulation generates a large amount of dynamical entanglement compared to non-modulating case which generates a low stationary entanglement. This study shows that in the future this sort of hybrid optomechanical device can be used for data signal transfer, storage and can become part of a broader quantum information processing unit.

### Acknowledgments

P.K Jha, Aranya B. Bhattacharjee and Vijay Bhatt are thankful to Department of Science and Technology DST(SERB), Project No. EMR/2017/001980, New Delhi for the financial support. Aranya B. Bhattacharjee and Souri Banerjee is grate-

ful to **BITS Pilani, Hyderabad campus** for the facilities to carry out this research.

---

- [1] F. Marquardt and S. M. Girvin, *Physics* **2**, **40** (2009).
- [2] M. Aspelmeyer, S. Groblacher, K. Hammerer, and N. Kiesel, *J. Opt. Soc. Am. B* **27**, A189 (2010).
- [3] T. J. Kippenberg and K. J. Vahala, *Opt. Express* **15**, 17172 (2007).
- [4] G. J. Milburn and M. J. Woolley, *Acta. Phys. Slov.* **61**, 5 (2012).
- [5] W. P. Bowen and G. J. Milburn, *Quantum optomechanics* (CRC press, 2015).
- [6] M. Aspelmeyer, T. J. Kippenberg, and F. Marquardt, *Cavity optomechanics: nano- and micromechanical resonators interacting with light* (Springer, 2014).
- [7] C. Genes, D. Vitali, P. Tombesi, S. Gigan, and M. Aspelmeyer, *Phys. Rev. A* **77**, 033804 (2008).
- [8] S. Groblacher et al., *Nat. Phys.* **5**, 485 (2009).
- [9] D. Vitali, S. Gigan, A. Ferreira, H. R. Bohm, P. Tombesi, A. Guerreiro, V. Vedral, A. Zeilinger, and M. Aspelmeyer, *Phys. Rev. Lett.* **98**, 030405 (2007).
- [10] E. Verhagen et al., *Nature (London)* **482**, **63** (2012).
- [11] J. Chan et al., *Nature (London)* **478**, **89** (2011).
- [12] A. Mari and J. Eisert, *Phys. Rev. Lett.* **103**, 213603 (2009).
- [13] A. Mari and J. Eisert, arXiv:1111.2415v1.
- [14] F. Galve, L. A. Pachon and D. Zueco, *Phys. Rev. Lett.* **105**, 180501 (2010).
- [15] M. J. Woolley, A. C. Doherty, G. J. Milburn, and K. C. Schwab, *Phys. Rev. A* **78**, 062303 (2008).
- [16] T. A. Palomaki, J. W. Harlow, J. D. Teufel, R. W. Simmonds, and K. W. Lehnert, *Nature (London)* **495**, 210 (2013).
- [17] A. H. Safavi-Naeini and O. Painter, *New J. Phys.* **13**, 013017 (2011).
- [18] K. Hammerer, M. Wallquist, C. Genes, M. Ludwig, F. Marquardt, P. Treutlein, P. Zoller, J. Ye, and H. J. Kimble, *Phys. Rev. Lett.* **103**, 063005 (2009).
- [19] M. Wallquist, K. Hammerer, P. Zoller, C. Genes, M. Ludwig, F. Marquardt, P. Treutlein, J.

- Ye, and H. J. Kimble, Phys. Rev. A **81**, 023816 (2010).
- [20] J. Johansson, P. Nation, F. Nori, Comput. Phys. Commun. **183**, 1760 (2012).
  - [21] M. A. Nielsen, I. L. Chuang, Quantum Computation and Quantum Information; Cambridge-University Press: Cambridge, 2000.
  - [22] M. Pinard, A. Dantan, D. Vitali, O. Arcizet, T. Briant, A. Heidmann, Europhys. Lett., **72**, 747 (2005).
  - [23] M. Paternostro, D. Vitali, S. Gigan, M. S. Kim, C. Brukner, J. Eisert, M. Aspelmeyer, Phys. Rev. Lett., **99** 250401 (2007).
  - [24] M. Bhattacharya, P. Meystre, Phys. Rev. Lett. **99** 073601 2007. M. Bhattacharya, H. Uys, P. Meystre, Phys. Rev. A **77**, 033819 (2008).
  - [25] C. Wipf, T. Corbitt, Y. Chen, N. Mavalvala, New J. Phys. **10**, 095017 (2008).
  - [26] D. Vitali, S. Gigan, A. Ferreira, H. R. Bhm, P. Tombesi, A. Guerreiro, V. Vedral, A. Zeilinger, M. Aspelmeyer, Phys. Rev. Lett., **98**, 030405 (2007).
  - [27] D. Vitali, S. Mancini, P. Tombesi, J. Phys.A. Math. Theor. **40**, 8055 (2007).
  - [28] S. Mancini, D. Vitali, P. Tombesi, Phys. Rev. Lett., **90**, 137901 (2003).
  - [29] S. Pirandola, S. Mancini, D. Vitali, P. Tombesi, J. Mod. Opt., **51**, 901 (2004).
  - [30] S. Pirandola, S. Mancini, D. Vitali, P. Tombesi, Phys. Rev. A, **68**, 062317 (2003).
  - [31] S. Pirandola, D. Vitali, P. Tombesi, S. Lloyd, Phys. Rev. Lett., **97**, 150403 (2006).
  - [32] M. Aspelmeyer, T. J. Kippenberg, and F. Marquardt, Rev. Mod. Phys. **86**, 1391 (2014).
  - [33] P. Meystre, Ann. Phys. (Berlin) **525**, 215 (2013).
  - [34] S. Chakraborty and A. K. Sarma Phys. Rev. A **97**, 022336 (2018).
  - [35] M. Abdi, Sh. Barzanjeh, P. Tombesi, and D. Vitali, Phys. Rev. A **84**, 032325 (2011).
  - [36] M. C. Kuzyk, S. J. Van Enk, H. Wang, Phys. Rev. A **88**, 062341 (2013).
  - [37] S. G. Hofer, W. Wieczorek, M. Aspelmeyer, and K. Hammerer, Phys. Rev. A **84**, 052327 (2011).
  - [38] G. Wang, L. Huang, Y.-C. Lai, and C. Grebogi, Phys. Rev. Lett. **112**, 110406 (2014).
  - [39] A. A. Rakhubovsky and R. Flipp, Phys. Rev. A **91**, 062317 (2015).
  - [40] B. Rogers, M. Paternostro, G. M. Palma, and G. De Chiara Phys. Rev. A **86**, 042323 (2012).
  - [41] X. -Z Yuan, Phys. Rev. A **88**, 052317 (2013).
  - [42] R. Blattmann, H. J. Krenner, S. Kohler, and P. Hanggi, Phys. Rev. A **89**, 012327 (2014).
  - [43] M. -C. Li and A. -X. Chen, Open Phys, **18**, 14-23 (2020).

- [44] J. Kabuss, A. Carmele, T. Brandes and A. Knorr, Phys. Rev. Lett. **109**, 054301 (2012).
- [45] A. Faraon, A. Majumdar, H. Kim, P. Petroff, and J. Vuckovic. arXiv:0906.0751v1, 2009.
- [46] A. Majumdar, A. Faraon, D. Englund, N. Manquest, H. Kim, P. Petroff, and J. Vuckovic Proc. SPIE 7611, Advances in Photonics of Quantum Computing, Memory, and Communication III, 76110L 2010; <https://doi.org/10.1117/12.843372>
- [47] C. U. Lei, A. J. Weinstein, J. Suh, E. E. Wollman, A. Kronwald, F. Marquardt, A. A. Clerk, and K. C. Schwab, Phys. Rev. Lett. **117**, 100801 (2016).
- [48] Y.- W. Hu, Y. -F. Xiao, Y. -C. Liu, Q. Gong, Front. Phys. **8(5)**: 475-490, (2013).
- [49] S. M. Thon, M. T. Rakher, H. Kim, J. Gudat, W. T. M. Irvine, P. M. Petroff, and D. Bouwmeester, Appl. Phys. Lett. **94**, 111115 (2009).
- [50] S. Mahajan and A. B. Bhattacharjee, Journal of Modern Optics, **66:6**, 652-664 (2019).
- [51] S. C. Wu, L. Zhang, J. Lu, L.-G. Qin and Z. -Y. Wang, arXiv:1909.12870v1 Sep. (2019).
- [52] M. K. Singh, P. K. Jha, A. B. Bhattacharjee, Optik, **185**, 685-691, (2019).
- [53] V. Bhatt, P. K. Jha, A. B. Bhattacharjee, Optik, **198**, (2019).
- [54] H. K. H. Choy, Design and fabrication of distributed Bragg reflectors for vertical-cavity surface-emitting lasers. M.Sc. Thesis, Mc Master University, (1996).
- [55] V. Giovannetti and D. Vitali, Phys. Rev. A **63**, 023812 (2001).
- [56] Y. C. Liu, Y. F. Shen, Q Gong and Y. F. Xiao, Physical Review A 89, 053821 (2014).
- [57] X. W. Xu and Y. Li, Phys. Review A **91**, 053854 (2015).
- [58] Y. Wu, I. M. Piper, M. Ediger, P. Brereton, E. R. Schmidgall, P. R. Eastham, M. Hugues, M. Hopkinson and R. T. Phillips, Phys. Rev. Lett. **106(6)**: 067401
- [59] V. S. Malinovsky and J. L. Krause Eur. Phys. J. D **14**, 147-155 (2001)
- [60] K. Bergmann, H. Theuer, and B.W. Shore, Rev. Mod. Phys. **70**, 1003 (1998).
- [61] A. Farace and V. Giovannetti, Phys. Rev. A **86**, 013820 (2012).
- [62] R. Horodecki, P. Horodecki, M. Horodecki, K. Horodecki, Quantum entanglement. Rev Mod Phys. **81(2)**, 865942 (2009).
- [63] HJ. Kimble, The quantum internet, Nature, **453(7198)** 102330 (2008).
- [64] P. Rabl, S. J. Kolkowitz, F. H. L. Koppens, J. G. E. Harris, P. Zoller, and M. D. Lukin, Nat. Phys. **6**, 602 (2010).
- [65] S. L. Braunstein and P. V. Lock, Rev. Mod. Phys. **77**, 513 (2005).
- [66] S. Mancini and P. Tombesi, Europhys. Lett. **61**, 8 (2003).

- [67] A. Xureb, C. Genes, and A. Dantan, Phys. Rev. Lett. **109**, 223601 (2012).
- [68] S. Ritter, C. Nolleke, C. Hahn, A. Reiserer, A. Neuzner, M. Uphoff, Nature, **484**(7393) :195200 (2012).
- [69] P. G. Kwiat, K. Mattle, H. Weinfurter, A. Zeilinger, A. V. Sergienko, Y. Shih, Phys Rev Lett. **75**(24) 433741 (1995).
- [70] W. P. Bowen, N. Treps, R. Schnabel, P. K. Lam, Phys Rev Lett. **89**(25) 253601 (2002).
- [71] J. D. Jost, J. P. Home, J. M. Amini, D. Hanneke, R. Ozeri, C. Langer, Nature, **459** (7247) 683-5 (2009).
- [72] E. Togan, Y. Chu, A. S. Trifonov, L. Jiang, J. Maze, L. Childress, Nature **466**(7307) 7304 (2010).
- [73] E. A. Sete, H. Eleuch, C. H. Raymond Ooi, Phys. Rev. A, **92**, 033843 (2015).
- [74] H. A. Boura, A. Rom. Isar, J. Phys., **60**, 1278 (2015)
- [75] S. L. Braunstein and P. V. Lock, Rev. Mod. Phys. **77**, 513 (2005).
- [76] G. Vidal and R. F. Werner, Phys. Rev. A **65**, 032314 (2002).
- [77] G. Adesso, A. Serani, and F. Illuminati, Phys. Rev. A **70**, 022318 (2004).
- [78] R. Simon, Phys. Rev. Lett. **84**, 2726 (2000).

## VII. APPENDIX A

Gaussian states are of central importance in the context of the continuous-variable (CV) quantum information. These are the states with Gaussian Wigner function and are characterized as well as solved entirely by the field quadrature operators' first and second moments [75]. Further, to discuss entanglement in CV systems, we consider a very prototypical CV entangled state, i.e., a two-mode Gaussian state. The following covariance matrix can represent this type of state,

$$V_2 = \begin{bmatrix} A & C \\ C^T & B \end{bmatrix}, \quad (\text{A1})$$

where A, B and C are  $2 \times 2$  block matrices which describe the local properties mode A, mode B and the intermode correlation between A and B. The continuous variable entangle-

ment between the two modes can be well calculated by using the logarithmic negativity  $E_N$  [76, 77] as,

$$E_N = \max[0, -\ln 2\nu^-]. \quad (\text{A2})$$

Where  $\nu^- = \left( \Sigma(V_2) - \sqrt{\Sigma(V_2)^2 - 4\det V_2} \right)^{1/2} 2^{-1/2}$  is the smallest symplectic eigenvalue of the partial transpose of  $V_2$  with  $\Sigma(V_2) = \det(A) + \det(B) - 2\det(C)$ . The Gaussian state is said to be entangled ( $E_N$ ) if it follow the Simon's necessary and sufficient nonpositive partial transpose criteria [78].